Journal for Geometry and Graphics
Volume — (2022), No. —, 1–15

On continuous flexible Kokotsakis belts of the isogonal type and V-hedra with skew faces*

Georg Nawratil

Institute of Discrete Mathematics and Geometry & Center for Geometry and Computational Design, TU Wien, Wiedner Hauptstraße 8-10/104, Vienna, Austria
nawratil@geometrie.tuwien.ac.at

Abstract. A. Kokotsakis studied the following problem in 1932: Given is a rigid closed polygonal line (planar or non-planar), which is surrounded by a polyhedral strip, where at each polygon vertex three faces meet. Determine the geometries of these closed strips with a continuous mobility. On the one side, we generalize this problem by allowing the faces, which are adjacent to polygon line-segments, to be skew; i.e to be non-planar. But on the other side, we restrict to the case where the four angles associated with each polygon vertex fulfill the so-called isogonality condition that both pairs of opposite angles are equal or supplementary. In more detail, we study the case where the polygonal line is a skew quad, as this corresponds to a (3×3) building block of a so-called V-hedron composed of skew quads. The latter also gives a partial answer to a question posed by R. Sauer in his book of 1970 whether continuous flexible skew quad surfaces exist.

Key Words: Kokotsakis belt, continuous flexibility, skew quad surfaces

MSC 2020: 51N05 (primary), 51M04, 51N15

1 Introduction

Let us consider a so-called Kokotsakis belt [11] illustrated in Fig. 1a, which can be defined as follows:

Definition 1. *The original Kokotsakis belt consists of a rigid closed polygonal line* p *(not necessarily planar) with n vertices $V_0,\dots,V_{n-1}$, which is surrounded by a belt of planar polygons in a way that each vertex V_i of* p *has valence four.*

In general these loop structures are rigid, thus continuous flexible ones possess a so-called over-constrained mobility. Kokotsakis himself formulated the problem for general rigid closed polygonal

*This is an extended version of [19] presented at the 20th International Conference on Geometry and Graphics.

ISSN 1433-8157/$ 2.50

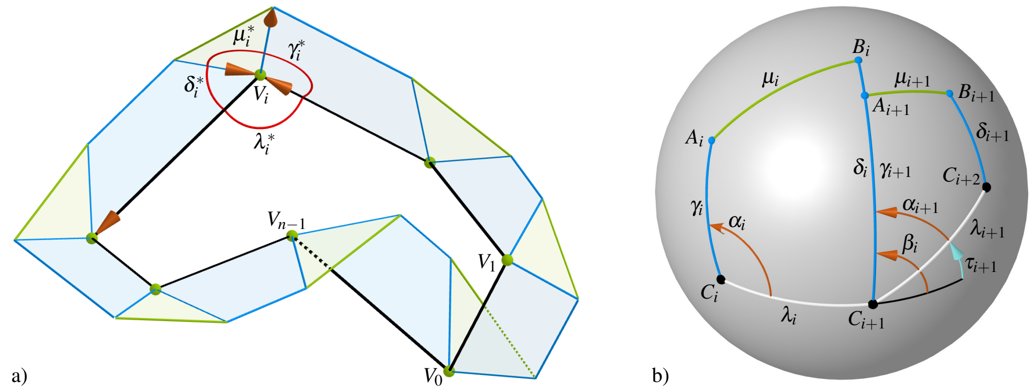

Figure 1: (a) Original Kokotsakis belt (cf. Def. 1) where the planar angles $\delta_i^*, \gamma_i^*, \lambda_i^*, \mu_i^* \in (0;\pi)$ are illustrated as well as the orientation of the enclosing line-segments used for the construction of the spherical image, which is illustrated in parts in (b). Note that the edge $V_{i-1}V_i$ is mapped to the point C_i.

lines p, but in fact he only studied flexible belts with planar polygons p in [11]. Planarity was only not assumed in the study of necessary and sufficient conditions for infinitesimal flexibility (see also Karpenkov [10]). Clearly, the restriction to planar polygons p makes sense in the context of continuous flexible polyhedra, as this condition has to be fulfilled around faces where all vertices have valence four[1].

Our interest in Kokotsakis belts results from our research on continuous flexible polyhedral surfaces; especially those composed of rigid planar quads in the combinatorics of a square grid. A very well known class of these flexible planar-quad (PQ) surfaces are *V-hedra*, which are the discrete analogs of Voss surfaces[2] according to [23]. They can easily be characterized by the fact that in each vertex the angles of opposite planar quads are equal. The question whether V-hedra can be generalized by dropping the planarity condition of the quads (cf. Fig. 2) motivated us for the study of so-called generalized Kokotsakis belts, which can be defined as follows:

Definition 2. *The generalized Kokotsakis belt is obtained from the original one given in Defnition 1 by dropping the planarity condition of the faces adjacent to the polygon line-segments of* p.

The article at hand is structured as follows: We proceed in Section 1.1 with a literature review on flexible Kokotsakis belts, where we place emphasis on the so-called isogonal type[3], which means that in every polygon vertex both pairs of opposite angles are (1) equal or (2) supplementary. In Section 2 we discuss the spherical image of Kokotsakis belts from a kinematical point of view. Based on these considerations we study generalized flexible Kokotsakis belts of the isogonal type in Section 3. In Section 4 we discuss continuous flexible skew-quad (SQ) surfaces, where we focus on V-hedra composed of skew quads in more detail. The paper is concluded in Section 5.

1.1 Review on continuous flexible Kokotsakis belts

Until now only examples of continuous flexible Kokotsakis belts are known where the rigid polygon line p is planar as well as all faces adjacent to its line-segments. Therefore these assumptions hold for the complete review section, which is structured along the number n of vertices $V_0, \ldots, V_{n-1}$ of p (cf. Fig. 1a).

---

[1] Assumed that this part of the continuous flexible polyhedra is not rigid.
[2] Surfaces on which geodesic lines form a conjugate curve network [29].
[3] This notation is in accordance with [26].

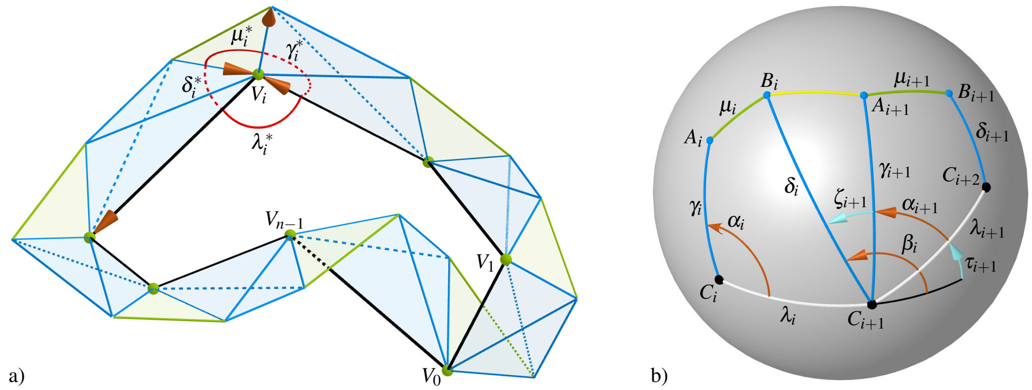

Figure 2: (a) Generalized Kokotsakis belt (cf. Def. 2) and a part of its corresponding spherical image (b).

General results (for all $n > 2$) were only obtained by Kokotsakis [11] for the isogonal type, to which for example rigidly foldable origami twists [5] belong as a special case. For $n = 3$ and $n = 4$ more results are known, which can be summarized as follows:

- **Case** $n = 3$**:** This case implies continuous flexible octahedra, which are very well studied objects dating back to Bricard [3]. Especially, the Bricard octahedra of the 3rd type (cf. [25]) correspond to the isogonal case, which was already pointed out by Kokotsakis [11]. Moreover, the study of these Kokotsakis belts allows also the determination of continuous flexible octahedra with vertices at infinity [16].

- **Case** $n = 4$**:** These Kokotsakis belts, which are also known as (3×3) complexes, are the building blocks of continuous flexible PQ surfaces according to [23, Theorem 3.2]. Based on spherical kinematic geometry [26], a partial classification of continuous flexible (3×3) building blocks was obtained by Stachel and the author [15, 17, 18]. Inspired by this approach, Izmestiev [8] obtained a full classification containing more than 20 cases.

  Note that the first classes of continuous flexible PQ surfaces were given by Sauer and Graf [21]; namely the so-called T-hedra (see also [22, 24]) and the already mentioned V-hedra (see also [14, 22]).

  A rigid-foldable PQ surface which can be developed is a special case of origami. Under the additional condition of flat-foldability (as in case of the popular Miura-ori) Tachi [27, 28] developed computational tools to design surfaces, where each vertex is of the isogonal type. Recently, Feng et al. [6] gave a complete analysis of the flat-foldable case, which can also be used for design tasks [4].

  Within the field of computational design Jiang et al. [9] presented recently an optimization technique to penalize an isometrically deformed surface with planar quads. Its design space is restricted to rigid-foldable quad-surfaces which can be seen as a discretization of flexible smooth surfaces (e.g. Voss surfaces, profile-affine surfaces [21, 22]).

Remark 1. *Note that for the cases $n > 4$ no specific results are known to the author.* ⋄

2 Spherical image of Kokotsakis belts

In order to get a consistent notation for the construction of the spherical image of the Kokotsakis belt we orient the line-segments meeting at a vertex V_i according to Figs. 1a and 2a, respectively.

Taking this orientation of the line-segments into account, the spherical 4-bar mechanism, which corresponds with the arrangement of faces around V_i, has the following spherical bar lengths:

$$\delta_i = \pi - \delta_i^*, \quad \gamma_i = \pi - \gamma_i^*, \quad \lambda_i = \pi - \lambda_i^*, \quad \mu_i = \pi - \mu_i^* \tag{1}$$

for the index[4] $i = 0, \ldots, n-1$. The spherical image of faces around two adjacent vertices V_i and V_{i+1} is illustrated in Figs. 1b and 2b, which show the motion transmission from the vertex C_i over C_{i+1} to C_{i+2} by two coupled spherical 4-bar mechanisms. Note that in the isogonal case these 4-bar mechanisms are so-called spherical isograms fulfilling one of the following two conditions:

$$(1) \quad \lambda_i = \mu_i, \quad \delta_i = \gamma_i, \qquad\qquad (2) \quad \lambda_i + \mu_i = \pi, \quad \delta_i + \gamma_i = \pi. \tag{2}$$

These two types are related by the replacement of one of the vertices of the spherical isogram by its antipodal point, which does not change its motion. In Section 3 we show that we can restrict to type (1) without loss of generality by assuming an appropriate choice of orientations. In the following we use the half-angle substitutions

$$\sin\alpha_i = \tfrac{2a_i}{1+a_i^2}, \quad \cos\alpha_i = \tfrac{1-a_i^2}{1+a_i^2}, \quad \sin\beta_i = \tfrac{2b_i}{1+b_i^2}, \quad \cos\beta_i = \tfrac{1-b_i^2}{1+b_i^2}, \tag{3}$$

in order to end up with algebraic expressions. It is well known (e.g. [26]) that the input angle α_i and the output angle β_i of the i-th spherical isogram of type (1) of Eq. (2) are related by

$$b_i = f_i a_i \quad \text{with} \quad f_i \neq 0 \quad \text{and} \qquad f_i = \tfrac{\sin\delta_i \pm \sin\lambda_i}{\sin(\delta_i - \lambda_i)}. \tag{4}$$

The two options in the expression for f_i implied by the $\pm$ sign refer to the case whether the motion transmission corresponds to that of a spherical parallelogram ($\Leftrightarrow f_i > 0$) or spherical antiparallelogram ($\Leftrightarrow f_i < 0$), respectively. Note that the degenerated cases ($\delta_i = \lambda_i$ and $\delta_i + \lambda_i = \pi$) of the spherical isogram are excluded by the condition $f_i \neq 0$ given in Eq. (4).

The angles β_i and α_{i+1} are related over the offset angle ε_{i+1}; i.e. $\beta_i + \varepsilon_{i+1} = \alpha_{i+1}$. This means that ε_{i+1} gives only the shift between the output angle β_i of the i-th isogram to the input angle α_{i+1} of the $(i+1)$-th isogram. This yields the relation:

$$\tan\alpha_{i+1} = \tfrac{\tan\beta_i + \tan\varepsilon_{i+1}}{1 - \tan\beta_i \tan\varepsilon_{i+1}}. \tag{5}$$

Using the half-angles and the Weierstrass substitution $e_{i+1} := \tan\frac{\varepsilon_{i+1}}{2}$ yield

$$a_{i+1} = \tfrac{b_i + e_{i+1}}{1 - b_i e_{i+1}}. \tag{6}$$

Note that the spherical arcs $B_iC_{i,i+1}$ and $A_{i+1}C_{i,i+1}$ enclose the *twist angle* $\zeta_{i+1} := \varepsilon_{i+1} + \tau_{i+1}$ (cf. Fig. 2b), where the latter angle is the *torsion angle* of the spatial polygon p, which is defined as the angle enclosed by the spherical arcs C_iC_{i+1} and $C_{i+1}C_{i+2}$. From the polygon p the angles τ_{i+1} can be computed as the angle of rotation about the oriented axis V_iV_{i+1}, which brings the plane $[V_{i-1}, V_i, V_{i+1}]$ to the plane $[V_i, V_{i+1}, V_{i+2}]$. Therefore the angle τ_{i+1}, which is within the interval $(-\pi;\pi]$, can be computed as:

$$\tau_{i+1} = \operatorname{sign}(o) \arccos\left(\tfrac{(c_i \times c_{i+1})(c_{i+1} \times c_{i+2})}{\|c_i \times c_{i+1}\| \|c_{i+1} \times c_{i+2}\|}\right) \quad \text{with} \quad o := (c_i \times c_{i+1})\, c_{i+2} \tag{7}$$

where c_i denotes the vector from V_{i-1} to V_i. Note that the $\operatorname{sign}(o)$ term is needed for orienting the angle τ_{i+1}.

Remark 2. *For the original Kokotsakis belt (cf. Fig. 1) the twist angle ζ_{i+1} is zero ($\Rightarrow \varepsilon_{i+1} = -\tau_{i+1}$) or π ($\Rightarrow \varepsilon_{i+1} = \pi - \tau_{i+1}$) for all $i = 0, \ldots, n-1$. Note that* p *is a planar curve if all τ_{i+1} are either zero or π.* ◇

[4] Note that in the remainder of the paper the indices are taken modulo n.

3 Continuous flexible Kokotsakis belts of the isogonal type

According to [26, Theorem 1] the Kokotsakis belt is continuous flexible if and only if the spherical image has this property. Now we will show that any Kokotsakis belt of the isoganal type can be identified with a spherical mechanism, which is only composed of spherical isograms of type (1) in Eq. (2):

We start with the spherical image of p, i.e. the points $C_0,\ldots,C_{n-1}$ and construct the spherical points A_0 and B_0 according to Section 2. If the spherical isogram $C_0C_1B_0A_0$ is of type (2) then we replace B_0 by its antipode. Then we proceed as follows around the spherical image of the polyline p; i.e. for $i=0,\ldots,n-1$:

a. In the case where the two antipodal points, which are candidates for A_{i+1}, correspond with the values zero and π for ε_{i+1}, we have to choose the one which implies $\varepsilon_{i+1}=0$ as $\varepsilon_{i+1}=\pi$ is not covered by Eq. (6). In any other case A_{i+1} can be chosen arbitrary from the corresponding set of two antipodal points.

b. B_{i+1} has to be chosen from the corresponding set of two antipodal points such that the spherical isogram $C_{i+1}C_{i+2}B_{i+1}A_{i+1}$ is of type (1).

We can end up in two situations; either $A_n=A_0$ and we are done or A_n is the antipodal point of A_0. In the latter case we denote by j the highest possible index within the set $\{0,\ldots,n-1\}$ for which the choice of A_{i+1} was done arbitrarily in step (a). Then we replace all A_{i+1} and B_{i+1} with $i\geq j$ by their antipodal points which yields $A_n=A_0$.

Note that such a j has to exist as otherwise we can construct the following contradiction: No j exists if and only if there are no shifts; i.e. $e_0=e_1=\ldots=e_{n-1}=0$. As a consequence $\alpha_0=\beta_0=0$ implies $\alpha_{i+1}=\beta_{i+1}=0$ for all $i\in\{0,\ldots,n-1\}$, which already shows that in this case $A_n=A_0$ has to hold.

As a consequence of the above considerations one can write down the condition for continuous flexibility of any Kokotsakis belt of the isogonal type, where the rigid polygon p has $n>2$ vertices, as

$$a_0-a_n=0. \tag{8}$$

In this so-called closure condition we substitute a_n by

$$a_i=\tfrac{a_{i-1}f_{i-1}+e_i}{1-a_{i-1}f_{i-1}e_i} \tag{9}$$

which results from Eq. (6) under consideration of Eq. (4). By iterating this substitution (in total n times) we end up with an expression of the form $q_2a_0^2+q_1a_0+q_0=0$ where q_2,q_1,q_0 are functions in $f_0,\ldots,f_{n-1},e_0,\ldots,e_{n-1}$. This means that the spherical coupler arms A_0C_0 and A_nC_0 coincide for all input angles α_0 if and only if the following necessary and sufficient conditions for continuous mobility are fulfilled:

$$q_2=0,\quad q_1=0,\quad q_0=0. \tag{10}$$

This result is needed for the proof of the following theorem:

Theorem 1. *For a given closed polygon* p *with n vertices, there exists at least a* $(2n-3)$*-dimensional set of continuous flexible Kokotsakis belts of the isogonal type over* $\mathbb{C}$.

Proof. The given polygon p already determines the angles λ_i and τ_i for $i=0,\ldots,n-1$. Therefore the $2n$ unknowns μ_i and ζ_i remain free, which have to fulfill the three equations of Eq. (10). □

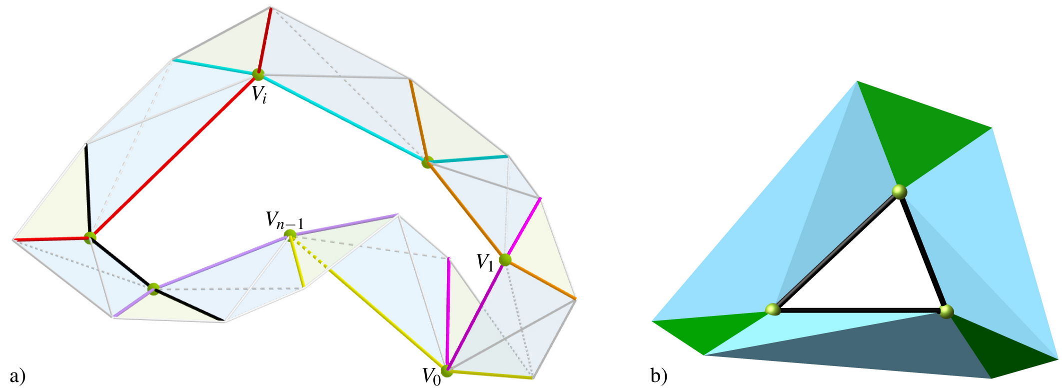

Figure 3: Generalized Kokotsakis belt of the isogonal type: (a) Edges with the same absolute values of their rotation angles during the continuous flexibility are illustrated with the same color. (b) For $n = 3$ we obtain an overconstrained angle-symmetric 6R linkage.

By taking a closer look at $q_2 = 0$ it can easily be seen that the terms linear in e_i are given by $f_0 e_1$ and $f_0 \dots f_{k-1} e_k$ for $k = 2, \dots, n$. In the equation $q_0 = 0$ the linear terms in e_i are e_0, $e_{n-1} f_{n-1}$ and $e_k f_k \dots f_{n-1}$ for $k = 1, \dots, n-2$. Therefore each of the two conditions $q_2 = 0$ and $q_0 = 0$ can only be fulfilled independently from the choice of the f_i's if there are no shifts; i.e. $e_0 = e_1 = \dots = e_{n-1} = 0$. Note that these are not only necessary conditions but already sufficient ones as they imply $q_2 = q_0 = 0$. In this case the remaining condition $q_1 = 0$ simplifies to $f_0 f_1 \cdots f_{n-1} = 1$ and we end up with a $(n-1)$-dimensional set of continuous flexible Kokotsakis belts of the isogonal type over $\mathbb{C}$. Note that $e_0 = e_1 = \dots = e_{n-1} = 0$ only implies planarity of p if we assume the faces to be planar. These considerations are needed for proving the second sentence of the following theorem:

Theorem 2. *For a given closed polygon p with $n > 3$ vertices, there exists at least a $(n-3)$-dimensional set of continuous flexible Kokotsakis belts with planar faces of the isogonal type over $\mathbb{C}$. For planar curves p (which is always true for $n = 3$) this dimension raises to $(n-1)$.*

Proof. For a spatial polyline p with planar faces the spherical coupler arms $B_i C_{i+1}$ and $A_{i+1} C_{i+1}$ are aligned. Therefore not only the angles λ_i and τ_i for $i = 0, \dots, n-1$ are determined but also ζ_i (cf. Remark 2). As a consequence we only remain with the n unknowns μ_i which have to meet the three conditions of Eq. (10). If p is planar then two of these three equations are already fulfilled identically as pointed out above. □

3.1 Property regarding the rotation angles

According to [11, §8] opposite angles in a spherical isogram are either equal or complete each other to 2π. As a consequence opposite dihedral angles along edges meeting in a vertex V_i have at each time instant t the same absolute value of their angular velocities. Therefore the absolute values of the rotation angles around these two edges are the same (measured from an initial starting configuration). As one of the dihedral angels is the angle about an edge $V_i V_{i+1}$ of the polygon p, this property holds for the two spherical 4-bars, which have the common point C_{i+1} (cf. Figs. 1b and 2b, respectively). Therefore the same absolute values of the rotation angle can always be assigned to three edges within a continuous flexible Kokotsakis belt of the isogonal type (cf. Fig. 3a).

Example 1. *Now we consider the case $n = 3$. For any choice of δ_i and γ_i for $i = 1, 2, 3$ and $\gamma_1 + \gamma_2 + \gamma_3 = 2\pi$ (closure condition of central triangle) there exist $e_0, e_1, e_2 \in \mathbb{C}$ such that we get a* *continuous flexible Kokotsakis belt of the isogonal type. The resulting structure can be seen as an overconstrained 6R loop (cf. Fig. 3b), which belongs to the third class of so-called angle-symmetric 6R linkages [12] due to the above discussed angle property. Note that for* $e_0 = e_1 = e_2 = 0$ *we get the already mentioned Bricard octahedron of type III (cf. case* $n = 3$ *in Section 1.1).* ◇

Remark 3. *In this context it should also be noted that the relative motion between two consecutive faces of a continuous flexible Kokotsakis belt of the isogonal type is rational. Therefore another approach towards this overconstrained mechanism could be based on the study of the motion of its spherical image by means of quaternions using techniques for the factorization of quaternionic motion polynomials [7, 20].* ◇

4 Continuous flexible SQ surfaces

On page 168 of Sauer's book [22] the following open problem is mentioned: *Do there exist continuous flexible SQ surfaces?* A key result for the answering of this question is the following generalization of Theorem 3.2 of [23]:

Theorem 3. *A non-degenerate SQ surface is continuous flexible, if and only if this holds true for every* (3×3) *building block.*

Proof. The arguments used for the proof of Theorem 3.2 of [23] do not rely on the planarity of the involved quads. □

Based on this result a partial answer to Sauer's question is given in Section 4.2.

4.1 Associated overconstrained mechanism

We start this section with the definition of reciprocal-parallel quad meshes:

Definition 3. *Two quad meshes* $\mathscr{Q}$ *and* $\mathscr{V}$ *are called reciprocal-parallel if the following conditions are fulfilled:*

- ⋆ $\mathscr{Q}$ *and* $\mathscr{V}$ *are combinatorial dual; i.e. vertices of one mesh correspond to the faces of the other and vice versa.*
- ⋆ *The edges of both meshes are related by the implied bijection that edges of adjacent faces are mapped to edges between corresponding adjacent vertices and vice versa.*
- ⋆ *Edges, which are related by this bijection, are parallel.*

Sauer [22] showed that every infinitesimal flexible quad surface $\mathscr{Q}$ possesses in general a unique (up to scaling) reciprocal-parallel quad mesh $\mathscr{V}$. The reciprocal-parallel surface of the latter mesh $\mathscr{V}$ is only uniquely determined (up to scaling) if $\mathscr{Q}$ is composed of skew quads, otherwise there exist infinitely many, which are in a parallelism relation[5] to each other (cf. [22, Theorem 16.22]).

The corresponding deformation of the $\mathscr{V}$ mesh during the continuous flexion of $\mathscr{Q}$ has to be a conformal transformation, as the vertex stars are rigid. The corresponding kinematic structure of $\mathscr{V}$ is composed of rigid vertex stars linked by cylindrical joints (cf. Fig. 5). Note that in general such a structure only has the trivial finite flexibility resulting from the homothetic transformation. This motion can be omitted by fixing the length of one edge in the structure. These modified linkages are in general rigid but those stemming from continuous flexible quad surfaces $\mathscr{Q}$ have an overconstrained motion.

[5] Corresponding faces and edges of these meshes are parallel.

4.2 V-hedra with skew quads

We study this class in more detail, as it is a generalization of V-hedra with planar quads having many applications to structural engineering practice [13, 14].

For $n=4$ the equations $q_2=q_1=q_0=0$ of Eq. (10) read as follows:

$$\begin{aligned}
q_2 :=&f_0[e_0f_3(e_1e_2f_2+e_2e_3f_1+e_1e_3-f_1f_2)+e_1e_2e_3f_2-e_3f_1f_2-e_2f_1-e_1],\\
q_1 :=&e_1e_2f_0f_2f_3+e_2e_3f_0f_1f_3+e_1e_3f_0f_3-e_1e_3f_1f_2-f_0f_1f_2f_3-e_1e_2f_1-e_2e_3f_2+1+\\
&e_0(e_1e_2e_3f_1f_3-e_1e_2e_3f_0f_2-e_1f_1f_2f_3+e_3f_0f_1f_2+e_2f_0f_1-e_2f_2f_3+e_1f_0-e_3f_3),\\
q_0 :=&e_0(e_1e_3f_1f_2+e_1e_2f_1+e_2e_3f_2-1)+f_3(e_1e_2e_3f_1-e_1f_1f_2-e_2f_2-e_3).
\end{aligned} \tag{11}$$

We can solve this set of equations explicitly for e_1,e_2,e_3 in dependence of $e_0,f_0,\ldots,f_3$, which yields the following two solutions:

$$\begin{aligned}
e_1 &= \frac{e_0f_0f_2(f_1^2-1)(f_3^2-1)\pm R_1R_2}{e_0^2(f_0f_2-f_1f_3)(f_0-f_1f_2f_3)+(f_0f_3-f_1f_2)(f_0f_2f_3-f_1)},\\
e_2 &= \frac{\mp R_1R_2}{e_0^2(f_0f_1-f_2f_3)(f_0f_2-f_1f_3)+(f_0f_1f_3-f_2)(f_0f_2f_3-f_1)},\\
e_3 &= \frac{e_0f_1f_3(f_0^2-1)(f_2^2-1)\pm R_1R_2}{e_0^2(f_0f_2-f_1f_3)(f_0f_1f_2-f_3)+(f_0f_3-f_1f_2)(f_0f_1f_3-f_2)}
\end{aligned} \tag{12}$$

with

$$\begin{aligned}
R_1 &:= \sqrt{e_0^2(f_0f_1-f_2f_3)(f_0f_2-f_1f_3)+(f_0f_1f_3-f_2)(f_0f_2f_3-f_1)},\\
R_2 &:= \sqrt{e_0^2(f_0f_1f_2-f_3)(f_1f_2f_3-f_0)+(f_0f_1f_2f_3-1)(f_1f_2-f_0f_3)}.
\end{aligned} \tag{13}$$

Remark 4. *Alternatively, the above given equations $q_2=q_1=q_0=0$ from Eq. (11) can also be solved explicitly for f_1,f_2,f_3 in dependence of $f_0,e_0,\ldots,e_3$, which yield the following two solutions:*

$$\begin{aligned}
f_1 &= \frac{-(f_0^2+1)e_0e_1(e_3^2+1)(e_2^2-1)+f_0(e_0^2e_1^2e_2^2-e_0^2e_1^2e_3^2-e_0^2e_2^2e_3^2-e_1^2e_2^2e_3^2+e_0^2+e_1^2+e_2^2-e_3^2)\pm R_+R_-}{2e_2(e_3^2+1)(e_0f_0+e_1)(e_0e_1-f_0)},\\
f_2 &= \frac{(f_0^2+1)e_0e_1(e_3^2+1)(e_2^2+1)-f_0(e_0^2e_1^2e_2^2+e_0^2e_1^2e_3^2-e_0^2e_2^2e_3^2-e_1^2e_2^2e_3^2-e_0^2-e_1^2+e_2^2+e_3^2)\mp R_+R_-}{2e_2e_3f_0(e_1^2+1)(e_0^2+1)},\\
f_3 &= \frac{-(f_0^2+1)e_0e_1(e_3^2-1)(e_2^2+1)-f_0(e_0^2e_1^2e_2^2-e_0^2e_1^2e_3^2+e_0^2e_2^2e_3^2+e_1^2e_2^2e_3^2-e_0^2+e_1^2+e_2^2-e_3^2)\pm R_+R_-}{2e_3(e_2^2+1)(e_1f_0+e_0)(e_0e_1-f_0)}
\end{aligned} \tag{14}$$

with

$$\begin{aligned}
R_\pm :=&[f_0(e_0^2e_1^2e_2^2+e_0^2e_1^2e_3^2-e_0^2e_2^2e_3^2-e_1^2e_2^2e_3^2-e_0^2-e_1^2+e_2^2+e_3^2)\\
&-(f_0^2+1)e_0e_1(e_3^2+1)(e_2^2+1)\pm 2f_0e_2e_3(e_1^2+1)(e_0^2+1)]^{\frac{1}{2}}.
\end{aligned} \tag{15}$$

◇

Note that for a given skew central quad p and a set of real values $e_0,\ldots,e_3,f_0,\ldots,f_3$ fulfilling the three equations $q_2=q_1=q_0=0$, the missing geometric parameters δ_i can be computed from the equation $\sin\delta_i \pm \sin\lambda_i - f_i\sin(\delta_i-\lambda_i)=0$ (cf. Eq. (4)). For the minus sign we get one further real solution beside the excluded degenerate case $\delta_i=\lambda_i$. By shifting these two values obtained for δ_i by π we obtain the solutions of the equation with respect to the plus sign. Therefore we get a unique value for $\delta_i\in(0;\pi)$ with $\delta_i\neq\lambda_i$ for each $i=0,\ldots,3$.

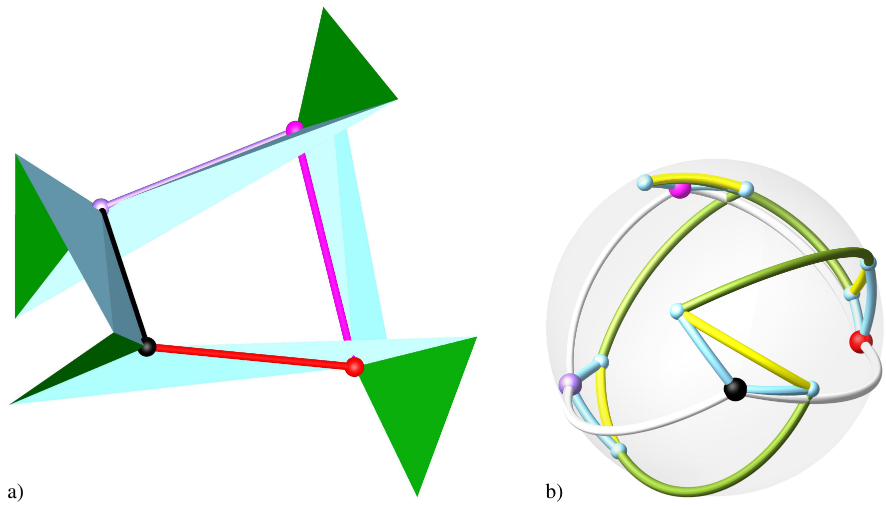

Figure 4: A (3×3) building block of a V-hedron with skew quads (a) and its spherical image (b). The vertex V_i and the line-segment $V_{i-1}V_i$ have the same color, where $i=0$ corresponds to black, $i=1$ to red, $i=2$ to magenta and $i=3$ to purple. Note that the illustrations of Figs. 4, 5 and 7 are rendered with respect to the same view. The animations of the mobility of the V-hedron and its spherical image are online available at `https://www.dmg.tuwien.ac.at/nawratil/skew_quad_spatial.gif` and `https://www.dmg.tuwien.ac.at/nawratil/skew_quad_spherical.gif`, respectively.

Remark 5. *Note that for each 8-tuple $e_0,\ldots,e_3,f_0,\ldots,f_3$ fulfilling the three equations $q_2=q_1=q_0=0$ a 5-dimensional set of continuous flexible (3×3) building blocks of V-hedra with skew quads can be associated. This is due to the fact that τ_i and λ_i (for $i=0,\ldots,3$) are not uniquely determined by $e_0,\ldots,e_3,f_0,\ldots,f_3$ and that the shape of the central skew quad is determined by 5 parameters, which can be seen as follows: Without loss of generality one can assume that the first vertex of the central quad equals the origin of the fixed frame (i.e. $V_0=(0,0,0)^T$), the second one is located on its x-axis (i.e. $V_1=(x_1,0,0)^T$), the third one belongs to the xy-plane (i.e. $V_2=(x_2,y_2,0)^T$) and the fourth vertex is unrestricted (i.e. $V_3=(x_3,y_3,z_3)^T$). This yields in total 6 parameters which reduces to 5 by canceling the factor of similarity (e.g. $x_1=1$).* ◇

Example 2. *The coordinates of the vertices of the skew central quad* p *are given by:*

$$V_0=(5,0,0)^T,\quad V_1=(4,3,0)^T,\quad V_2=(1,2,2)^T,\quad V_3=(0,0,0)^T, \tag{16}$$

from which the angles λ_i and τ_i for $i=0,\ldots,3$ can be calculated. Moreover, the input data is completed by the values:

$$e_0=100,\quad d_0=0.3,\quad d_1=0.15,\quad d_2=0.2,\quad d_3=0.25, \tag{17}$$

where $d_i=\tan\frac{\delta_i}{2}$. From that we can compute the f_i values according to Eq. (4) with respect to the minus sign for all $i=0,\ldots,3$. Then the formulas for the solution set related to the upper sign in Eq. (12) yield

$$e_1=-0.86081001,\quad e_2=-5.06077939,\quad e_3=0.57043281. \tag{18}$$

One configuration of the resulting continuous flexible (3×3) building block of a V-hedron with skew quads is illustrated in Fig. 4, where also the corresponding spherical image is displayed. The *associated overconstrained mechanism implied by the reciprocal-parallelism (cf. Section 4.1) is shown in Fig. 5. In the captions of Figs. 4 and 5 we also provide links to* `gif` *animations showing the overconstrained motion of these three mechanisms.* ◇

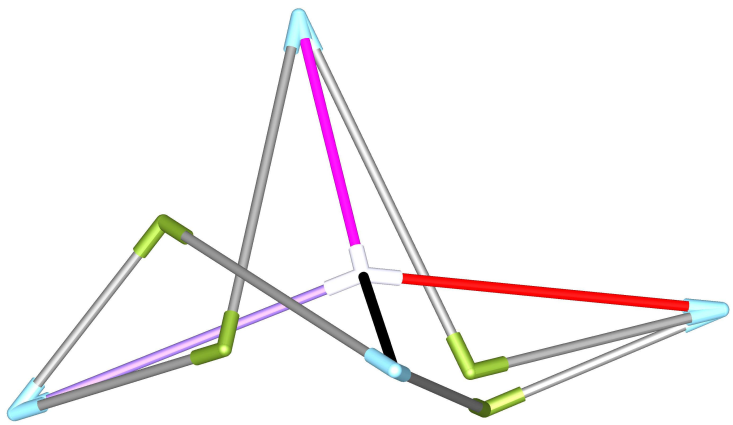

Figure 5: The overconstrained mechanism which results from the reciprocal-parallelism to the (3×3) building block of a V-hedron with skew quads illustrated in Fig. 4a. The animation of the mobility of this mechanism is online available at `https://www.dmg.tuwien.ac.at/nawratil/skew_quad_reciprocal.gif`, where we fixed the length of the black edge, which is parallel to V_3V_0.

4.2.1 Lower bound on the dimension of the design space

A lower bound on the dimension of the design space of continuous flexible V-hedra with skew quads can be obtained by comparing the number q_{par} of essential free parameters for constructing a $([3+t]\times[3+s])$ skew quad mesh at the one hand-side with the number q_{con} of algebraic conditions needed to make the mesh isogonal and continuous flexible. We do this count of parameters and conditions in three steps illustrated in Fig. 6; in step (i) we consider a (3×3) building block, in step (ii) we add to it s columns and in step (iii) we extend the $(3\times[3+s])$ complex by t rows. In order to improve the clarity of the approach we label the vertices by double indices; i.e. by $V_{\text{row,column}}$.

i. Let us start with a non-planar quad with vertices $V_{1,1}$, $V_{1,2}$, $V_{2,2}$ and $V_{2,1}$. Its shape (up to scaling) is determined by 5 parameters according to Remark 5. Now one can add to each of the four vertices two edges, where each has 2 free degrees for orientation, in order to get an arrangement of a (3×3) building block (cf. Fig. 6i), which therefore has $5+2\cdot 8=21$ parameters.

   Beside the three conditions $q_2=q_1=q_0=0$ in each of the four vertices the isogonality criterion has to hold, which can be expressed by two algebraic equations. This gives in total $3+2\cdot 4=11$ conditions for the arrangement of Fig. 6i to have a continuous flexibility of the isogonal type.

ii. Now we add a column to the building block. First we add a vertex on each of the two edges in the third column of Fig. 6ii. For each of these points $V_{1,3}$ and $V_{2,3}$ we have one free parameter. In each of the two vertices we add again two edges, where each has 2 free degrees for orientation. Therefore the adding of a column implies $2+2\cdot 4=10$ extra parameters.

   On the other side, in each of the two vertices $V_{1,3}$ and $V_{2,3}$ the isogonality condition has to hold and the (3×3) complex with center quad $V_{1,2}V_{1,3}V_{2,3}V_{2,2}$ has to fulfill the three conditions $q_2=q_1=q_0=0$. Thus the adding of a column increases the number by conditions by $3+2\cdot 2=7$.

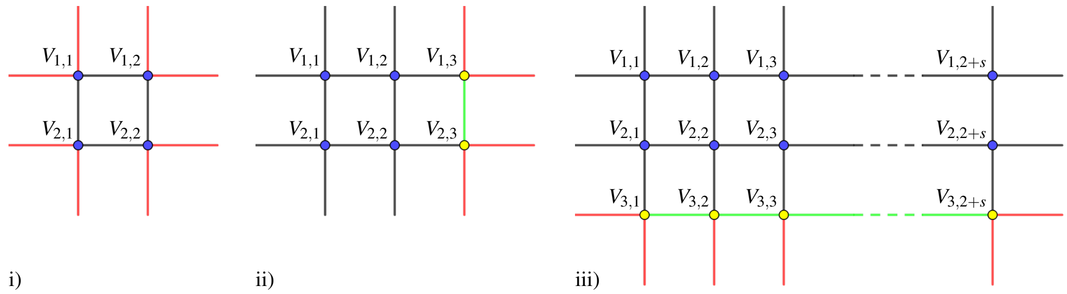

Figure 6: Schematic sketch of the construction of a $([3+t]\times[3+s])$ V-hedron with skew quads. The red color of the edges indicates that their adding implies 2 free degrees for orientation. The yellow color of the vertices expresses that one has 1 free degree for its selection on the black edge. The green colored edges imply no additional degree of freedom as they are already determined by the two adjacent yellow vertices.

iii. Now we add a row to the $(3\times[3+s])$ complex. We add a vertex on each of the edges in the third row of Fig. 6iii. For each of these $2+s$ vertices $V_{3,1}$, $V_{3,2}$, $\ldots$, $V_{3,2+s}$ there exists one degree of freedom for the selection on the respective edge. Moreover, in each of the $2+s$ new vertices we add one vertical edges, where each has 2 free degrees for orientation. Only in the first vertex $V_{3,1}$ and last vertex $V_{3,2+s}$ we can additional add a horizontal edge. Therefore the adding of a row implies $(2+s)+2\cdot(2+s)+2\cdot 2=10+3s$ extra parameters.

   In each of the $2+s$ vertices the isogonality criterion has to hold. In addition $1+s$ new (3×3) complexes can be identified (where the vertices of the center quads are $V_{2,i}V_{2,i+1}V_{3,i+1}V_{3,i}$ for $i=1,\ldots,1+s$), where each one has to fulfill the three conditions $q_2=q_1=q_0=0$. Thus the extension by a row implies $2\cdot(2+s)+3\cdot(1+s)=7+5s$ additional conditions.

From these considerations the numbers q_{par} and q_{con} can be computed as:

$$\begin{aligned} q_{par} &= 21+10s+(10+3s)t = 21+10s+10t+3st,\\ q_{con} &= 11+7s+(7+5s)t = 11+7s+7t+5st. \end{aligned} \tag{19}$$

Thus finally we get the lower bound[6] q on the dimension of the design space of continuous flexible $([3+t]\times[3+s])$ V-hedra with skew quads by

$$q := q_{par}-q_{con}-1 = 9+3s+3t-2st. \tag{20}$$

The subtraction of 1 comes from the fact that the structure has a 1-dimensional mobility; i.e. a 1-dimensional set of configurations is associated with one design. The values of q in dependence of s and t are printed in the symmetric Table 1. This table and Example 2 also give a partial answer to the question posed by Robert Sauer whether continuous flexible SQ surfaces exist (over $\mathbb{C}$). It remains open if such a structure of infinite dimension in rows and columns exists.

Remark 6. *Doing a similar count for V-hedron with planar quads one ends up with $q=6+2s+2t$, where the edges $V_{1,i}V_{1,i+1}$ for $i=1,\ldots,1+s$ as well as $V_{j,1}V_{j+1,1}$ for $j=1,\ldots,1+t$ can be assumed to be of unit length (without loss of generality) in order to reduce to the essential set of free parameters.* $\diamond$

[6] Every irreducible component of the intersection of m affine hypersurfaces $\in\mathbb{C}^n$ is at least of dimension $n-m$.

t\s	0	1	2	3	4	5	6	7	8	9	10	11	12	13	14	15	$i>15$
0	9	12	15	18	21	24	27	30	33	36	39	42	45	48	51	54	9+3i
1		13	14	15	16	17	18	19	20	21	22	23	24	25	26	27	12+i
2			13	12	11	10	9	8	7	6	5	4	3	2	1	0	<0
3				9	6	3	0	<0	<0	<0	<0	<0	<0	<0	<0	<0	<0
4					1	<0	<0	<0	<0	<0	<0	<0	<0	<0	<0	<0	<0
5						<0	<0	<0	<0	<0	<0	<0	<0	<0	<0	<0	<0
$\vdots$							$\ddots$	$\ddots$	$\ddots$	$\ddots$	$\ddots$	$\ddots$	$\ddots$	$\ddots$	$\ddots$	$\ddots$	$\vdots$

Table 1: Lower bound on the dimension of the design space of continuous flexible $([3+t]\times[3+s])$ V-hedra with skew quads.

4.2.2 Final comments

We close this section by making the following two final comments:

- The edges of the V-hedron can be subdivided into two families of discrete parameter lines, which are called u-polylines and v-polylines for short. Due to the property pointed out in Section 3.1, the rotation angles along any u-polyline or v-polyline are the same. Note that this property is well known for V-hedra with planar quads (cf. [21, page 529]) but also holds for the skew case.

- In view of Section 4.1 it should be noted that there is a further remarkable relation to an overconstrained mechanism beside the one illustrated in Fig. 5. As already pointed out by Sauer [22] the vertex star fulfilling the isogonality condition is reciprocal-parallel to a skew isogram, which has the following additional property: If the four bars of the isogram are hinged in the vertices by rotational joints, which are orthogonal to the plane spanned by the linked bars (cf. Fig. 7), then one obtains a so-called Bennett mechanism [2]. This is the only non-trivial mobile 4R loop.

  If the quads of the V-hedron $\mathscr{Q}$ are skew then the four axes of the Bennett mechanisms, which can be associated with a vertex of the mesh $\mathscr{V}$, differ from each other (cf. Fig. 7). Only in the case where $\mathscr{Q}$ is a V-hedron with planar quads, each vertex of $\mathscr{V}$ can uniquely be associated with one rotational axis orthogonal to the planar vertex star. Then the resulting network of Bennett mechanisms is highly mobile[7]. Finally it should be noted that in this case $\mathscr{V}$ is a discrete pseudospherical surface [22, 23, 30].

5 Conclusions, open problems and future research

We generalized continuous flexible Kokotsakis belts of the isogonal type by allowing that the faces, which are adjacent to the line-segments of the rigid closed polygon p, to be skew. In more detail we studied the case where p is a skew quad (SQ) as it corresponds to a (3×3) building block of a V-hedron composed of skew quads, which gives a partial answer to the question posed by Robert Sauer whether continuous flexible SQ surfaces exist. It remains an open problem if such a structure of infinite dimension in rows and columns exists. Moreover it would be interesting to check cases with a low value for q given in Table 1 (i.e. SQ meshes of size (7×7), (6×9) and (5×18), respectively) for the existence of real solutions by means of a numerical algebraic software

[7]The degree of the mobility corresponds to the number of rows plus columns of $\mathscr{V}$ minus one (cf. Sauer [22, Theorem 11.18]).

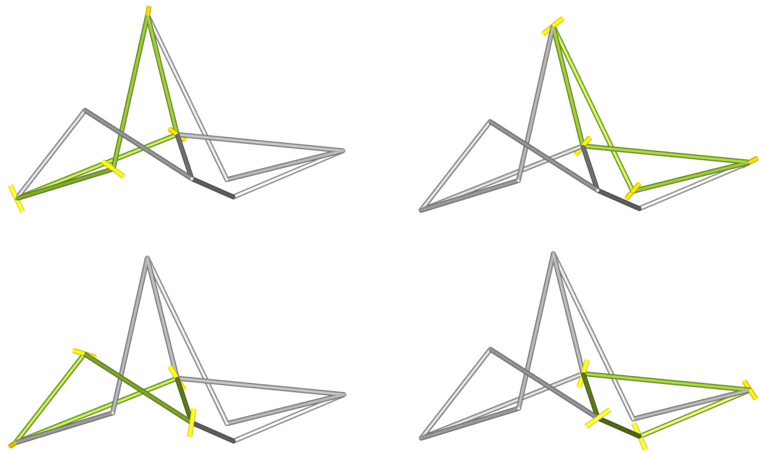

Figure 7: The four Bennett mechanisms associated with the structure illustrated in Fig. 5, where the rotation axes are displayed in yellow.

(e.g. Bertini [1]). Moreover, this tool could also be used to look for irreducible components with a higher dimension than q, whose geometric properties may imply continuous flexible SQ surfaces of infinite size in rows and columns.

Further open questions regard the smooth analog of continuous flexible Kokotsakis belts of the isogonal type and of V-hedra with skew quads. This study at hand is also the starting point towards a full classification of continuous flexible (3×3) SQ building blocks, which is subject to future research.

Acknowledgements

The research is supported by grant F77 (SFB "Advanced Computational Design", subproject SP7) of the Austrian Science Fund FWF.

References

[1] D.J. Bates, J.D. Hauenstein, A.J. Sommese, C.W. Wampler: *Bertini: Software for numerical algebraic geometry.* Available at bertini.nd.edu with permanent doi:dx.doi.org/10.7274/R0H41PB5

[2] G.T. Bennett: *The skew isogram mechanism.* Proceedings of the London Mathematical Society **s2-13**(1):151–173 (1914)

[3] R. Bricard: *Mémoire sur la théorie de l'octaèdre articulé.* Journal de Mathématiques pures et appliquées, Liouville **3**:113–148 (1897)

[4] X. Dang, F. Feng, P. Plucinsky, R.D. James, H. Duan, J. Wang: *Inverse design of deployable origami structures that approximate a general surface.* International Journal of Solids and Structures **234-235**:111224 (2022)

[5] T.A. Evans, R.J. Lang, S.P. Magleby, L.L. Howell: *Rigidly foldable origami twists.* Origami^6, I: Mathematics (K. Miura et al. eds.), pp. 119–130, American Mathematical Society (2015)

[6] F. Feng, X. Dang, R.D. James, P. Plucinsky: *The designs and deformations of rigidly and flat-foldable quadrilateral mesh origami.* Journal of the Mechanics and Physics of Solids **142**:104018 (2020)

[7] G. Hegedüs, J. Schicho, H.-P. Schröcker: *Factorization of rational curves in the Study quadric and revolute linkages.* Mechanism and Machine Theory **69**:142–152 (2013)

[8] I. Izmestiev: *Classification of flexible Kokotsakis polyhedra with quadrangular base.* International Mathematics Research Notices **2017**(3):715–808 (2017)

[9] C. Jiang, H. Wang, V.C. Inza, F. Dellinger, F. Rist, J. Wallner, H. Pottmann: *Using isometries for computational design and fabrication.* ACM Transactions on Graphics **40**(4):42 (2021)

[10] O.N. Karpenkov: *On the flexibility of Kokotsakis meshes.* Geometriae Dedicata **147**:15–28 (2010)

[11] A. Kokotsakis: *Über bewegliche Polyeder.* Mathematische Annalen **107**:627–647 (1932)

[12] Z. Li, J. Schicho: *Classification of angle-symmetric 6R linkages.* Mechanism and Machine Theory **70**:372–379 (2013)

[13] T. Mitchell, A. Mazurek, C. Hartz, M. Miki, W. Baker: *Structural Applications of the Graphic Statics and Static-Kinematic Dualities: Rigid Origami, Self-Centering Cable Nets, and Linkage Meshes.* Proceedings of the IASS Annual Symposium (July 16-20, 2018, Boston/USA), Symposium: Graphic statics, pp. 1-8(8) (2018)

[14] N. Montagne, C. Douthe, X. Tellier, C. Fivet, O. Baverel: *Voss surfaces: a design space for geodesic gridshells.* Journal of the International Association for Shell and Spatial Structures **61**(206):255–263 (2020)

[15] G. Nawratil, H. Stachel: *Composition of spherical four-bar-mechanisms.* New Trends in Mechanisms Science – Analysis and Design (D. Pisla et al. eds.), pp. 99–106, Springer (2010)

[16] G. Nawratil: *Flexible octahedra in the projective extension of the Euclidean 3-space.* Journal for Geometry and Graphics **14**(2):147–169 (2010)

[17] G. Nawratil: *Reducible compositions of spherical four-bar linkages with a spherical coupler component.* Mechanism and Machine Theory **46**(5):725–742 (2011)

[18] G. Nawratil: *Reducible compositions of spherical four-bar linkages without a spherical coupler component.* Mechanism and Machine Theory **49**:87–103 (2012)

[19] G. Nawratil: *Generalizing Continuous Flexible Kokotsakis Belts of the Isogonal Type.* ICGG 2022 – Proceedings of the 20th International Conference on Geometry and Graphics (L.-Y. Cheng ed.), pp. 115–126, Springer (2023)

[20] I. Niven: *Equations in quaternions.* The American Mathematical Monthly **48**(10):654–661 (1941)

[21] R. Sauer, H. Graf: *Über Flächenverbiegung in Analogie zur Verknickung offener Facettenflache.* Mathematische Annalen **105**:499–535 (1931)

[22] R. SAUER: *Differenzengeometrie.* Springer (1970)

[23] W.K. SCHIEF, A.I. BOBENKO, T. HOFFMANN: *On the integrability of infinitesimal and finite deformations of polyhedral surfaces.* Discrete Differential Geometry (A.I. Bobenko et al. eds.), Oberwolfach Seminars **38**:67–93 (2008)

[24] K. SHARIFMOGHADDAM, G. NAWRATIL, A. RASOULZADEH, J. TERVOOREN: *Using Flexible Trapezoidal Quad-Surfaces for Transformable Design.* Proceedings of IASS Annual Symposia, IASS 2020/21 Surrey Symposium: Transformable structures (IASS WG 15), pp. 1–13 (2021)

[25] H. STACHEL: *Remarks on Bricard's flexible octahedra of type 3.* Proceedings of the 10th International Conference on Geometry and Graphics (July 28 - Aug. 3, 2002, Kiev/Ukraine), **1**:8–12 (2002)

[26] H. STACHEL: *A kinematic approach to Kokotsakis meshes.* Computer Aided Geometric Design **27**:428–437 (2010)

[27] T. TACHI: *Generalization of rigid foldable quadrilateral mesh origami.* Journal of the International Association for Shell and Spatial Structures **50**(3):173–179 (2009)

[28] T. TACHI: *Freeform Rigid-Foldable Structure using Bidirectionally Flat-Foldable Planar Quadrilateral Mesh.* Advances in Architectural Geometry (C. Ceccato et al. eds.), pp. 87–102, Springer (2010)

[29] A. VOSS: *Über diejenigen Flächen, auf denen geodätische Linien ein konjugiertes System bilden.* Münchner Berichte, pp. 95–102 (1888)

[30] W. WUNDERLICH: *Zur Differenzengeometrie der Flächen konstanter negativer Krümmung.* Sitzungsbericht der Österreichischen Akademie der Wissenschaften, Mathem.-Naturw. Klasse IIa **160**(1-5):39–77 (1951)